Mesophase pitch-based high performance carbon fiber production using coal extracts from mild direct coal liquefaction

Christina Thompson[a, b*], George Frank[a, c], Vivian Edwards[a], Michela Martinelli[a], Asmund Vego[a], Frederic Vautard[d], Ercan Cakmak[d], John Craddock[a], Mark Meier[b], Rodney Andrews[a, c], Matthew Weisenberger[a, c]

[a]Center for Applied Energy Research, University of Kentucky, 2540 Research Park Drive, Lexington, KY, 40511, USA

[b]Department of Chemistry, University of Kentucky, Lexington, KY, 40506, USA

[c]Department of Chemical and Materials Engineering, University of Kentucky, Lexington, KY 40506, USA

[d]Oak Ridge National Laboratory, 1 Bethel Valley Road, Oak Ridge, TN 37831, USA

*christina.thompson16@uky.edu

Abstract

Mild direct coal liquefaction (autogenous pressure, no catalyst, no H_2 gas) of Springfield coal in fluid catalytic cracking decant oil is shown to effectively produce coal extract precursors to spinnable mesophase pitch. This work demonstrates that the coal extract can be thermally treated to obtain mesophase pitch in a facile one-step process, bypassing the production of an intermediate isotropic pitch. Furthermore, the presence of 25 wt.% coal in the initial slurry can increase the yield to mesophase pitch nearly twofold and yield to carbon fiber by approximately 70%. The coal extract-derived mesophase pitch was melt-spun and heat treated to produce carbon fiber with graphitic texture, high modulus (>400 GPa) and tensile strength up to 943 MPa. Overall, this work demonstrates that coal can be effectively utilized to markedly amplify the mesophase pitch and carbon fiber yield from fluid catalytic cracking decant oil by relatively simple processing, while conserving utility as a precursor to high performance carbon fiber and potentially other high value graphitic products.

Keywords: Coal, direct coal liquefaction, mesophase pitch, carbon fiber

1. Introduction

Carbon fiber has garnered much interest as a composite reinforcement material in the automotive, aerospace, civil infrastructure, and wind energy industries due to its high tensile strength, high stiffness, low coefficient of thermal expansion and low density. [1-3] While mesophase pitch-based carbon fiber makes up a very small fraction (<4%) of the commercial carbon fiber

market, it can offer higher modulus and higher carbonization yield than polyacrylonitrile (PAN)-based carbon fiber. [3, 4] The high modulus is a result of the alignment of relatively long-range and ordered graphitic domains along the fiber axis. This alignment is a result of the flow orientation that is conferred to a high optical texture index mesophase pitch precursor during the spinning process that produces green (unstabilized) fiber. Mesophase pitch can be obtained from various natural and synthetic aromatic feedstocks, with widespread precursors stemming from petroleum or coal tar isotropic pitches. [5, 6] Additionally, hydrogenated hypercoal has been shown to be an effective precursor for mesophase pitch and carbon fiber. [7] However, the direct utilization of abundantly available coal for carbon fiber production provides an attractive alternative to purely petroleum-based precursors due to potentially lower precursor cost and higher carbon yield. [8] Moreover, fluid catalytic cracking decant oil (DO), a known industrial precursor to mesophase pitch, is already in high demand as a precursor to needle coke and synthetic graphite.

Efforts have recently increased to utilize coal as a carbon ore for the production of value-added products to make use of the abundant natural resource while minimizing the impact of carbon emissions associated with coal combustion for electric power generation. [9] Utilizing coal as a feedstock for advanced carbon products such as carbon fiber is attractive because coal is a relatively low-cost feedstock material rich in polycyclic aromatic hydrocarbons (PAHs). Direct coal liquefaction (DCL) has been a key strategy within coal-to-products research as a method of breaking down the complex and highly cross-linked molecular structure of coal via solvolysis and hydrogenation. [10, 11] Numerous pure and commercial solvents have been examined to determine the relationship between solvent chemical structure and DCL coal conversion efficiency. [11-14]

Herein, a mild DCL process is employed with relatively low temperature and pressure, but in the absence of hydrogen gas or added catalysts. [15] Mild DCL is less energy-intensive and requires lower cost equipment due to the possibility of processing at pressures of several hundred, rather than thousand, psi. [16] Furthermore, mild DCL conditions limit excessive hydrocracking reactions to retain larger, less volatile compounds for improved carbon yield. [15] In this work, DO was chosen as the DCL solvent because it is a well-known industrial precursor to mesophase pitch with relatively low softening point temperature and desirable optical texture. [17-20] DO has been previously established as an effective coal liquefaction solvent for the production of fuels and anode coke. [15, 21] Using DO as a DCL solvent also offers an economic advantage due to its

relatively low cost compared to pure organic solvents, such as tetrahydronaphthalene (THN) and N-methyl pyrrolidone (NMP). It should be noted that while DO acts as a solvent during coal liquefaction, it is not subsequently recovered fully because it significantly participates in converting to mesophase and contributes to final carbon yield. However, distillate recovered during mesophase pitch production has potential utility as a recycle solvent in the DCL process, thus lowering the overall need for fresh DO.

Ultimately, this work describes the production of high modulus carbon fiber utilizing coal via the production of mesophase pitch from coal extracts obtained from mild DCL. The solvent fraction composition, molecular weight distribution, and heteroatom content of the coal extract is described and compared to that of DO. Quinoline insoluble (QI) matter was removed from the coal extract via solvent dilution and filtration, wherein tetrahydrofuran (THF) was found to be a superior solvent for coal extract recovery compared to toluene. A single-step thermal treatment of the filtered coal extract was then performed to produce a melt-spinnable mesophase pitch. The effective utilization of coal was shown to nearly double the yield to mesophase pitch and, moreover, increase yield to carbon fiber by approximately 70% compared to decant oil alone at similar processing conditions. The mesophase pitch-based carbon fiber showed high modulus (>400 GPa) and no cracking “Pac-man” defects.

2. Experimental

2.1 Materials

Springfield coal (SF) is a high volatile C bituminous coal (Western Kentucky No. 9, U.S.A.) and was chosen as a model beneficiated steam grade coal traditionally used for electric power generation. SF coal has an ash content of 6.61 wt. % (dry basis) and has been previously characterized in detail, including proximate and ultimate analysis, by Cakmak et al. [13] SF coal was pulverized and sieved to below 74 μm particle size (200 mesh) prior to use. Fluid catalytic cracking decant oil (DO) filtered to 0.2 μm was used as-received.

2.2 Coal extract production and conversion to mesophase pitch

An overview of the mesophase pitch production process is given in Figure 1. Mild direct coal liquefaction was carried out by loading SF coal and DO (1:3 by mass) into an autoclave and holding at 400 °C for 30 minutes under autogenous pressure (<450 psi) while stirring at 340 rpm.

These DCL conditions were previously optimized and determined to result in 76% coal conversion to quinoline solubles (dry, ash-free basis). [13] Additionally, DO alone was subjected to identical DCL conditions without the addition of coal, denoted DO*, to provide a baseline comparison for mesophase pitch production.

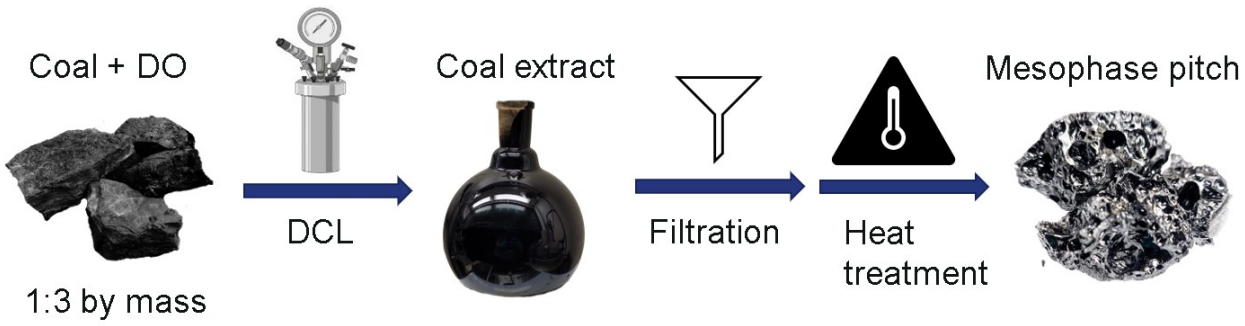

Figure 1. Overview process diagram of mesophase pitch production.

The obtained coal extract was filtered to remove quinoline insoluble matter, such as mineral matter initially present in the coal. Due to the high viscosity of SFDO, filtration methods using toluene and tetrahydrofuran (THF) dilution were investigated. Filtration using toluene as a diluent was conducted by dissolving SFDO in toluene at a 1:1 (toluene:SFDO) ratio by volume and vacuum filtering through a glass microfiber GF/D filter paper. Toluene was subsequently removed via rotary evaporation to afford the toluene soluble fraction of SFDO, designated SFDO-TS. Filtration with THF was conducted in a similar manner to obtain the THF soluble fraction (SFDO-THFS). The recovered diluent may be recycled for further reuse in this process.

Conversion of SFDO-TS and SFDO-THFS to mesophase pitch was carried out in a glass flask fitted in a heating mantle. Filtered SFDO was heated and held at an average temperature of 410 °C for 3 hours while stirring at 200 rpm with a N_2 purge through the overhead of the flask to prevent oxidation and to promote removal of volatiles from the system. DO* was processed in a similar manner for 3.5 hours. The mesophase pitch was allowed to cool under flowing nitrogen atmosphere, with stirring maintained while the viscosity of the mesophase pitch was sufficiently low. Mesophase pitch samples are designated by their precursor name followed by -MP.

2.3 Carbon fiber production

Mesophase pitch was melt spun into green fiber in a similar manner to that previously reported for production of general purpose carbon fiber from isotropic pitches derived from waste coal.[23] The mesophase pitch was heated to at least 50 ºC above its softening point in a small steel pressure vessel and extruded by N_2 overpressure through a bottom-mounted, single-hole spinneret (100 µm, L/D = 5, 120º entry angle) equipped with a 20 µm sintered stainless steel filter prior to the capillary hole. Real-time green fiber diameter was determined using a Keyence LS-7601 laser micrometer and the take-up spool speed was adjusted accordingly to obtain the desired fiber diameter.

Green fiber samples were oxidized by slowly ramping to approximately 300 ºC and holding isothermally on the order of ten minutes. The oxidatively stabilized fibers were carbonized and graphitized in a Thermal Technology LLC 1000-3060-FP20 graphite resistance furnace under flowing helium. The temperature was ramped to approximately 1000 ºC and held for tens of minutes, followed by ramping to greater than 2000 ºC. Graphitized fibers are designated by their precursor name followed by -CF.

2.4 Characterization

The procedure for determining quinoline insoluble content was adapted from ASTM D2318-20. Approximately 1 g of precursor sample was dissolved in 20 mL of quinoline and heated to 100 °C for approximately 1 hour while stirring. The mixture was then vacuum filtered through a glass microfiber GF/D filter paper (2.7 µm pore size). The filter cake was subsequently rinsed with tetrahydrofuran (THF) to remove residual quinoline and dried in a vacuum oven overnight. Solubility of mesophase pitch in toluene, pyridine, and quinoline was determined in a similar fashion, but due to its relatively low solubility, approximately 0.2 g of powdered sample was dissolved in 30 mL of solvent and stirred at 100 °C overnight. Only the quinoline insoluble filter cake was washed with THF, and all filter cakes were dried in a vacuum oven overnight.

Sulfur content of DO and SFDO was determined using a LECO S632 elemental analyzer according to ASTM standard D4239-18. Oxygen content was determined with an Elementar rapid OXY cube analyzer equipped with an infrared (IR) detector.

^{1}H nuclear magnetic resonance spectroscopy (^{1}H-NMR) was conducted on a 500 MHz JEOL ECZr equipped with a Royal Probe. Samples were dissolved in deuterated carbon disulfide and 1,4-dioxane-d8. The hydrogen distribution details the relative content of aromatic (H_{ar}, 9.0–6.0 ppm), methylene bridge (H_f, 4.5–3.3 ppm), naphthenic (H_n, 2.0–1.4 ppm), and aliphatic hydrogen in the α, β, and γ positions (H_α, 3.3–2.0; H_β, 1.4–1.0; H_γ, 1.0–0.5 ppm).[24-26] The average alkyl side chain length (n) was calculated as the ratio of integrations of total aliphatic hydrogen (H_α, H_β, H_γ) to hydrogen in the alpha position (H_α).[27]

Coal liquefaction products can be broadly separated into solubility classes: oils, asphaltenes and preasphaltenes.[28, 29] The relative content of oils, asphaltenes, and preasphaltenes in DO, DO*, and unfiltered SFDO was quantified by determining solubility fractions in heptane, toluene, and THF. Approximately 1 g of sample was dissolved in 20 mL of heptane and heated to 80 °C while stirring for approximately 1 hour. The mixture was then filtered through a glass microfiber GF/D filter paper and dried in a vacuum oven overnight. The difference between the initial SFDO mass and the mass of the dry filter cake is the mass of the oil fraction. Similarly, the heptane insolubles were dissolved in 20 mL of toluene, and the procedure was repeated to determine the heptane insoluble, toluene soluble fraction (asphaltenes). Finally, the heptane and toluene insolubles were dissolved in 20 mL of THF and stirred at room temperature, and the procedure was repeated to determine the heptane and toluene insoluble, THF soluble fraction (preasphaltenes).

Gel permeation chromatography (GPC) was carried out on an Agilent 1260 Infinity II GPC/SEC equipped with two Agilent Mesopore columns. N-methyl-2-pyrrolidone (NMP) was used as the eluent at a flow rate of 0.8 mL/min and a constant temperature of 60 °C. GPC chromatograms were obtained using a UV-visible diode array detector (DAD) at an absorption wavelength of 270 nm. Polystyrene and select PAH standards were used to obtain a calibration curve for determination of sample molecular weight.

The softening point temperature (T_{sp}) of mesophase pitch samples was determined using a TA Instruments DMA 850 according to ASTM E1545-22 Procedure B. The mesophase pitch was pelletized and mounted in a compression clamp that applied a constant force of 0.1 N while heating to 400 °C at a ramp rate of 5 °C/min.

Thermogravimetric analysis of mesophase pitch samples was conducted on a TA instruments TGA 5500 using a heating rate of 2 °C/min to 450 °C in 10 mL/min air flow to examine reactivity under conditions similar to those encountered during green fiber stabilization.

Reflected light polarized optical microscopy was conducted by examining mesophase pitch mounted in an epoxy puck with a Leitz Wetzlar microscope equipped with a polarizing filter. Volume percentage of anisotropic content was determined by a 1000-point count according to ASTM standard D4616-95.

Graphitized carbon fiber tensile properties were determined following ASTM standard D3379-75 via single filament tensile testing with compliance correction performed at gauge lengths of 10–50 mm.

To characterize the carbon fibers' surface and cross-section, scanning electron microscopy (SEM) was conducted using a TESCAN MIRA3 field emission microscope in secondary electron mode. The pristine graphitized fibers were cut with a fresh razor blade and secured on a sample holder with carbon tape prior to observation. The acceleration voltage was 10 kV, the beam intensity was set to 10, and the working distance was 10 mm.

To characterize carbon fiber structure, continuous θ-2θ X-ray diffraction (XRD) scans were performed on a PANalytical X'pert diffractometer with CuKα radiation (λ = 1.540598 Å). A parallel beam setup was used for these measurements with an incident beam side X-ray mirror and a 0.09° parallel plate collimator on the detector side. The fibers were finely chopped with a razor blade prior to these measurements to reduce the effects of preferred orientation. To calculate the crystallite sizes, the peak profiles were fitted using a Pearson VII profile function. To account for instrumental broadening, a full width at half maximum (FWHM) calibration curve was obtained using peak profile fits from a LaB_6 standard. The crystallite sizes (τ) were calculated using a Scherrer constant (K) of 0.9 for L_c according to the Scherrer Equation, Eq. (1):

$$\tau = \frac{K\lambda}{\beta \cos\theta} \tag{1}$$

Where, β is the FWHM after subtracting the instrumental FWHM, in radians, and θ is the Bragg angle. For L_c, the (002) reflection was used and the calculations were performed using the Jade software. Fitted profiles are shown in Figure S1-3.

3. Results and Discussion

3.1 Analysis of coal extract

SFDO was found to contain 5.79 wt. % QI, which is in reasonable agreement with the findings from microreactor studies of DCL of SF coal in DO at the same mass ratio and processing conditions reported by Cakmak et al. [13] QI content in SFDO is attributed to the mineral matter and insoluble organic matter (IOM) present in SF coal. As expected, oxygen and sulfur content was notably higher in SFDO relative to DO (Table 1).

Table 1. Sulfur and oxygen content (wt. %) of DO and SFDO.

	S	O
DO	0.08	0.42
SFDO	0.51	1.86

The relative hydrogen distribution obtained from ^{1}H-NMR spectroscopy is similar for DO before and after being subjected to DCL conditions without coal (DO*) (Table 2). On the other hand, the hydrogen distribution of SFDO differs in several aspects. A relative increase in naphthenic hydrogen (H_n) is observed, which may be due to the presence of naphthenic ring structures known to exist in bituminous coals. [30, 31] The apparent increase in H_β may be indicative of cleavage and subsequent H-capping of short alkane, ether or thioether bridges between aromatic groups during mild DCL. [31-33] These structural features may subsequently account for the increase in H_{al}/H_{ar} and average alkyl chain length (n) in SFDO.

Table 2. Hydrogen distributions of DO, DO*, and SFDO.

Sample	H_{ar}	H_f	H_n	H_α	H_β	H_γ	H_{al}/H_{ar}	n
DO	28.4	2.2	8.4	28.5	18.7	13.7	2.5	2.1
DO*	28.6	2.1	8.2	28.4	18.5	14.2	2.5	2.2
SFDO	26.4	2.1	10.4	25.9	21.2	14.0	2.8	2.4

Aromatic hydrogen (H_{ar}, 9.0–6.0 ppm), aliphatic hydrogen in methylene bridge α to two aromatic rings (H_f, 4.5–3.3 ppm), naphthenic hydrogen (H_n, 2.0–1.4 ppm), and aliphatic hydrogen in the α, β, and γ positions (H_α, 3.3–2.0 ppm; H_β, 1.4–1.0 ppm; H_γ, 1.0–0.5 ppm). Average alkyl chain length (n) is calculated as $(H_\alpha + H_\beta + H_\gamma)/ H_\alpha$.

Solvent fraction compositions (wt. %) of DO and SFDO are shown in Table 3. DO is composed primarily of oils (97%). Subjecting DO to DCL conditions without coal (DO*) had a

minimal effect on the solvent fraction composition. On the other hand, SFDO contains significantly higher content of asphaltenes and preasphaltenes. Although DO comprises 75% of the initial slurry, SFDO is only 67% oils, suggesting that oils are partially converted to asphaltenes due to reacting with coal during DCL processing. Indeed, the sum of the oil and asphaltene fractions (77%) is similar to the initial DO content (75%) in the slurry. Conversely, since SF coal makes up 25% of the initial slurry, this suggests that soluble material extracted from the coal is primarily in the form of preasphaltenes. Preasphaltenes are the most polar and highest molecular weight fraction, and therefore account for the marked increase in heteroatom content. [34] Finally, the remaining residue is THF insoluble (THFI).

Table 3. Solvent fraction composition and insoluble residue (wt. %) in DO, DO* and SFDO.

	Oils	Asphaltenes	Preasphaltenes	THFI
DO	97.0	3.0	-	-
DO*	95.3	4.4	-	-
SFDO	66.5	10.0	8.7	13.8

GPC/SEC analysis shows that the highest intensity peak of DO lies within approximately the 90-390 Da range, corresponding to a retention time (r.t.) of 20-24 minutes (Figure 2(a)). A slight increase in molecular weight was observed in DO* due to thermal condensation reactions occurring under DCL processing conditions. The extraction of high molecular weight species from SF coal during DCL is clearly observed in the molecular weight distributions of SFDO compared to DO*. Therefore, the shoulder region between approximately 950-5500 Da (r.t. 14-18 min) can primarily be attributed to coal-derived preasphaltenes. Additionally, species excluded from the column are observed at the peak at r.t ~10 min. The presence of excluded species is well documented for coal-derived materials and has been attributed to complex three-dimensional conformations of high molecular weight species as well as to preasphaltene aggregation. [35-38] Preasphaltenes are known to be prone to aggregation due to hydrogen bonding and acid-base interactions, even in dilute solutions. [34, 39, 40]

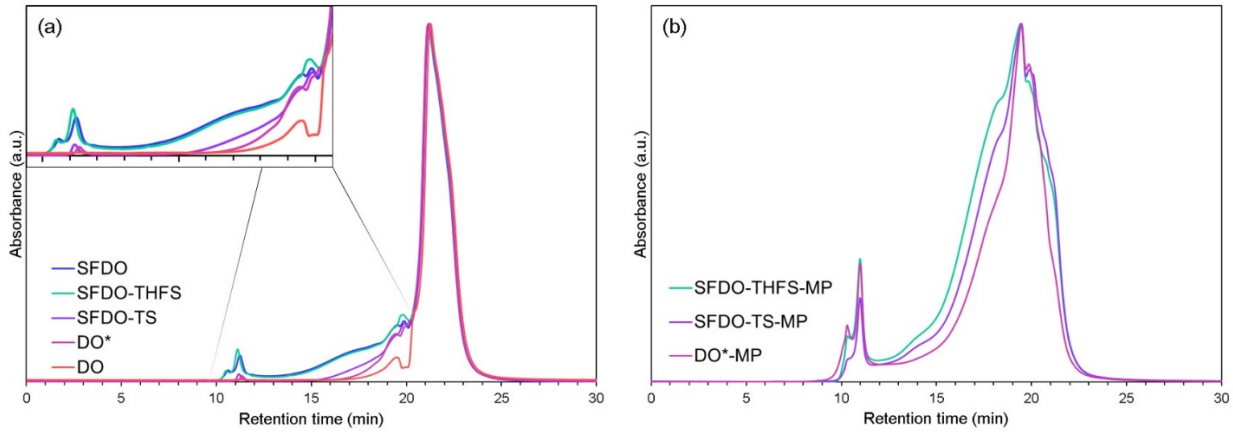

Figure 2. (a) Normalized GPC chromatograms of SFDO, SFDO-THFS, SFDO-TS, DO*, and DO. (b) Normalized GPC chromatograms of SFDO-THFS-MP, SFDO-TS-MP, and DO*-MP.

Filtration of the coal extract is necessary to remove insoluble residue, such as mineral matter and IOM, prior to thermal conversion to mesophase pitch. It has been well-established that the presence of QI has negative effects on mesophase formation and coalescence. [41-43] Filtration of SFDO diluted with solvent was shown to effectively reduce QI content to below 0.15 wt.% (Table S1). However, the choice of solvent diluent significantly alters the coal extract filtrate composition by acting as de facto solvent fractionation. Filtration with toluene dilution affords the toluene soluble fraction of SFDO (SFDO-TS), thereby removing preasphaltenes. The exclusion of preasphaltenes is observed in the GPC/SEC chromatograms due to the reduction in intensity corresponding to species in the ~950-5500 Da (r.t.14-18 mins) range (Figure 2). On the other hand, THF effectively dissolves preasphaltenes and therefore allows for higher recovery yield of filtered SFDO. This is confirmed by GPC where unfiltered SFDO and SFDO-THFS show nearly identical molecular weight distributions (Figure 2).

3.2 Coal extract-derived mesophase pitch

Mesophase pitches were produced from the filtered SFDO coal extracts via a one-step thermal treatment approach without the production of an intermediate isotropic pitch. It should be noted that mesophase pitch previously produced from similar coal extracts via an isotropic pitch intermediate did not have properties suitable for melt-spinning due to high T_{sp}. [22] The production of isotropic pitch from coal extracts involved vacuum distillation to reduce volatile matter content and therefore obtain a solid pitch. [22] However, bypassing distillation allows for the initial inclusion

of lower molecular weight species which lower the viscosity of the system, which is known to be favorable for mesophase formation by facilitating stacking of mesogens. [42, 44]

The molecular weight distributions of the NMP-soluble fraction of the mesophase pitches are shown in Figure 2(b). Compared to the molecular weight distributions of the precursors, the mesophase pitches show a relative decrease in intensity in the range of ~90-390 Da (r.t. 20-24 min), which is a result of the removal of more volatile components during thermal treatment. Both mesophase pitches stemming from coal extracts show broader molecular weight distributions and a greater intensity at higher molecular weights, which is consistent with the trends observed for the precursors.

The softening point and anisotropic content of SFDO-TS-MP and SFDO-THFS-MP are reported in Table 4 and compared to that of DO*-MP. DO*-MP showed complete conversion to mesophase with a relatively low T_{sp} below 300 ºC. Both SFDO-TS-MP and SFDO-THFS-MP show a significantly higher T_{sp} in comparison. However, SFDO-TS and SFDO-THFS show a striking improvement in thermal treatment yield to mesophase pitch compared to DO*. Both observations may be attributed to the increased presence of asphaltene and preasphaltene fractions in SFDO. [45-47] Additionally, the mesophase pitch solubilities in toluene, pyridine, and quinoline were determined (Table 4). The mesophase pitches reported here show similar solubilities to previously reported spinnable mesophase pitches. [19, 48] As anisotropy increases, a consistent decrease in solubility is observed, which is consistent with previous works. [49-51] Generally, literature suggests that higher pitch solubility corresponds to lower T_{sp}. [52-54] However, such a trend is not observed here because the mesophase pitches are derived from chemically distinct precursors and have different anisotropic contents.

Table 4. General properties of mesophase pitches derived from DO*, SFDO-TS and SFDO-THFS.

	T_{sp} (°C)	Anisotropy (%)	Thermal treatment yield (wt.%)	TI[1] (wt.%)	PI[2] (wt.%)	QI (wt.%)
DO*-MP	293	100	11.5	87.4	80.3	74.3
SFDO-TS-MP	331	90	18.0	80.9	64.5	50.6
SFDO-THFS-MP	321	93	21.7	86.5	66.6	51.4

[1]Toluene insoluble [2]Pyridine insoluble

Both SFDO-TS-MP and SFDO-THFS-MP showed ≥90% anisotropy with coalesced mesophase domains, which is beneficial for melt-spinning (Figure 3). [55] Furthermore, isotropic inclusions are relatively small (~10 μm diameter) and are homogenously distributed within the mesophase. Excessive phase separation of isotropic regions within mesophase pitch can negatively affect rheological homogeneity, and in turn result in poor spinning stability. [56, 57] Interestingly, SFDO-THFS-MP showed relatively large optical domains despite the inclusion of preasphaltenes, which have been previously reported to form mesophase with small optical domains compared to asphaltene and oil solvent fractions. [58-60] This reduction in optical domain size is likely related to higher molecular weight, heteroatom content, and resulting higher viscosity. [42, 61, 62] This ability of SFDO-THFS to form coalesced mesophase may be explained by a phenomenon similar to the dominant partner effect proposed by Marsh and others, which describes the inclusion of species which do not otherwise readily form mesophase being incorporated into a more fluid system without catastrophic detriment to mesophase formation. [42, 63, 64] That is, the DO-derived species control the optical texture of the mesophase pitch by adding fluidity to the system, allowing the formation of mesophase despite the inclusion of preasphaltenes. This phenomenon is critical for achieving a mesophase pitch with properties amenable to melt spinning while utilizing coal to achieve improved carbonization yield.

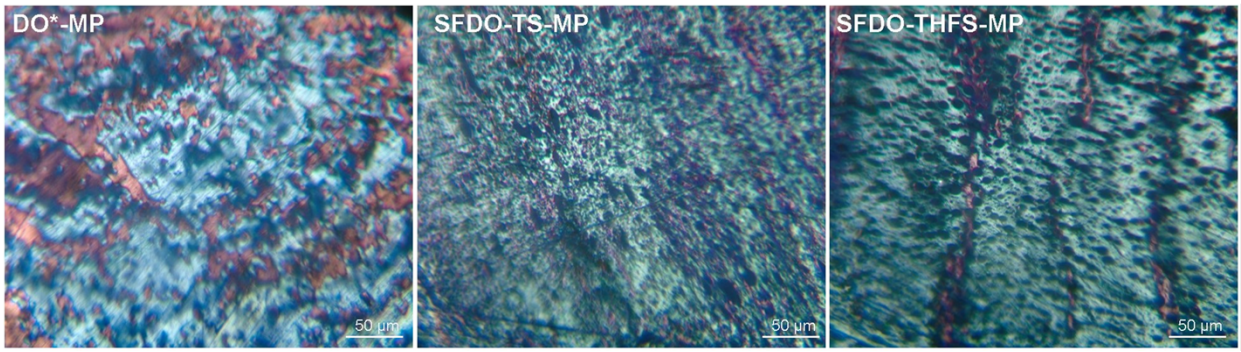

Figure 3. Polarized optical microscopy images of DO*-MP, SFDO-TS-MP, and SFDO-THFS-MP.

Thermogravimetric analysis of the mesophase pitches was conducted in air to gain insight into differences in reactivity of the carbon fiber precursors under conditions similar to green fiber stabilization procedures (Figure 4). All of the examined mesophase pitches exhibit net mass gain beginning at around 200 ºC, which is consistent with onset temperatures previously described for mesophase pitch green fibers under similar oxidation conditions. [65] DO*-MP displayed the most

rapid uptake of oxygen compared to both SFDO-derived mesophase pitches. DO*-MP, SFDO-TS-MP, and SFDO-THFS-MP reached maximum mass gain at approximately 350 ºC, 340 ºC, and 330 ºC, respectively. The differences in reactivity may be related to the already increased oxygen content of SFDO-derived precursors relative to DO alone.

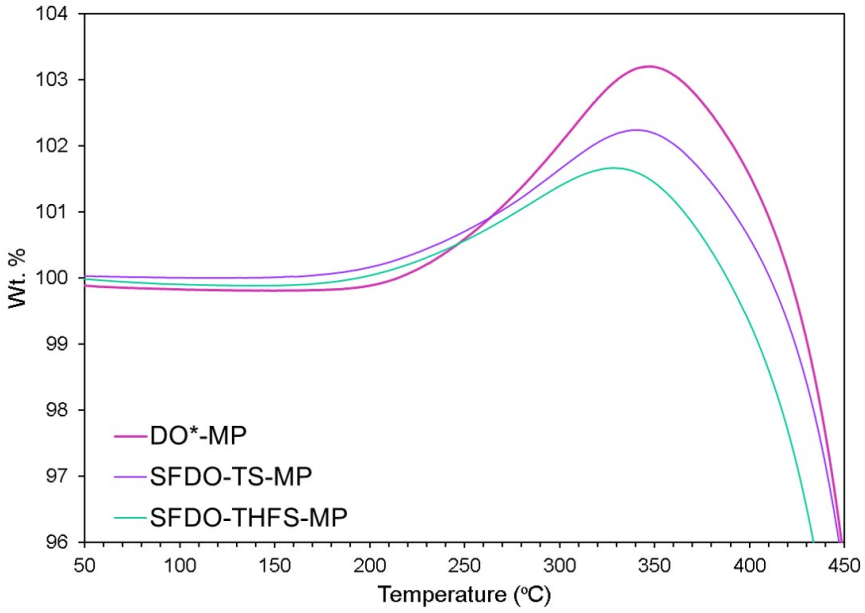

Figure 4. TGA curves of DO*-MP, SFDO-TS-MP, and SFDO-THFS-MP in air.

To demonstrate significant coal utilization, the overall mass yield to mesophase pitch and carbon fiber relative to initial slurry mass should be higher for coal extracts than that of processed DO alone. Therefore, DO was subjected to DCL conditions without coal, filtered, and thermally treated to produce a spinnable mesophase pitch and subsequently carbon fiber (DO*-CF). Mass yields of individual processing steps and replicates are given in Table S2-4. Overall yields to mesophase pitch were calculated as the product of filtered liquid recovery and thermal treatment yield (Figure 5). Compared to DO*-MP, SFDO-TS-MP did not show a notable improvement in overall yield despite a higher yield of SFDO-TS at the thermal treatment step, due to the low filtration yield as a result of preasphaltene insolubility. On the other hand, overall yield to SFDO-THFS-MP is nearly two-fold higher than DO*-MP. Overall yields to carbon fiber were calculated as the product of overall yield to mesophase pitch and the yield from green to graphitized fiber (Figure 5). Again, no significant difference in yield was observed between DO*-CF and SFDO-TS-CF. However, SFDO-THFS-CF showed approximately a 70% increase in overall yield to

carbon fiber relative to DO*-CF. This remarkable result showcases that the incorporation of preasphaltenes extracted from the coal is critical for efficient coal utilization in the final carbon products.

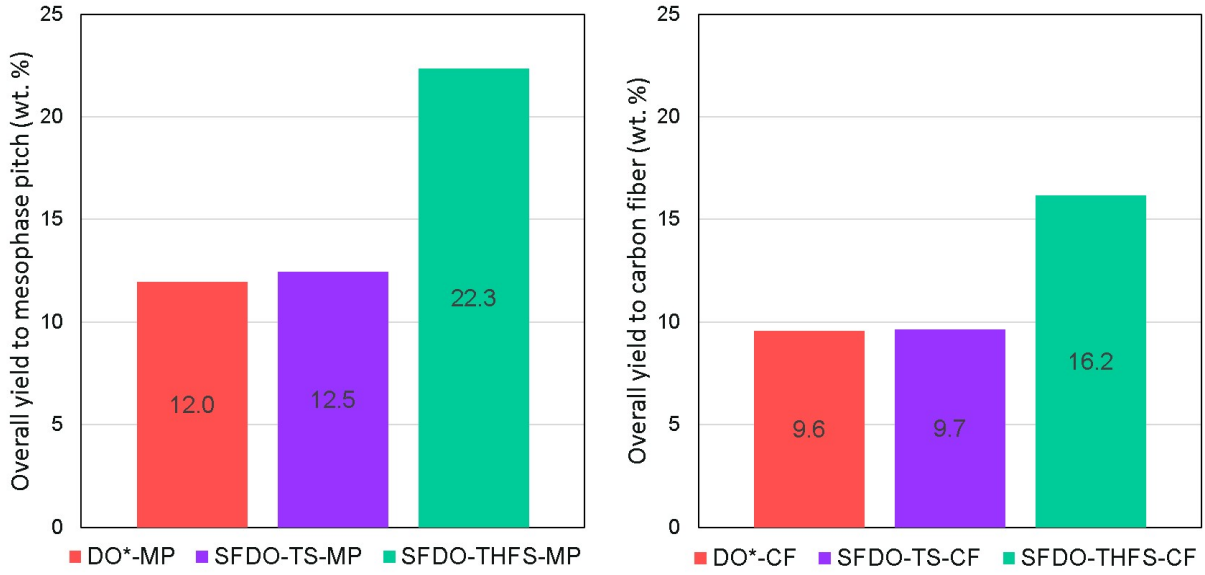

Figure 5. Overall mass yields to mesophase pitch (left) and to carbon fiber (right) derived from DO*, SFDO-TS, and SFDO-THFS.

3.4 Coal extract-derived carbon fiber

The obtained mesophase pitches were melt-spun into green fiber targeting approximately 30 µm diameter. Melt-spinning temperatures are listed in Table S5. The green fibers were subsequently oxidized, carbonized, and graphitized to obtain carbon fiber (Figure 6). Some variations in graphitic texture were observed, with both random and radial folded textures being present within the samples. Additional SEM images of graphitized fiber cross-sections and surfaces are given in Figure S4. No "Pac-man" splitting defects were observed, which is consistent with previous findings that small diameters, non-radial textures, and smaller crystallite sizes are associated with fewer cracking defects during fiber heat treatment. [66]

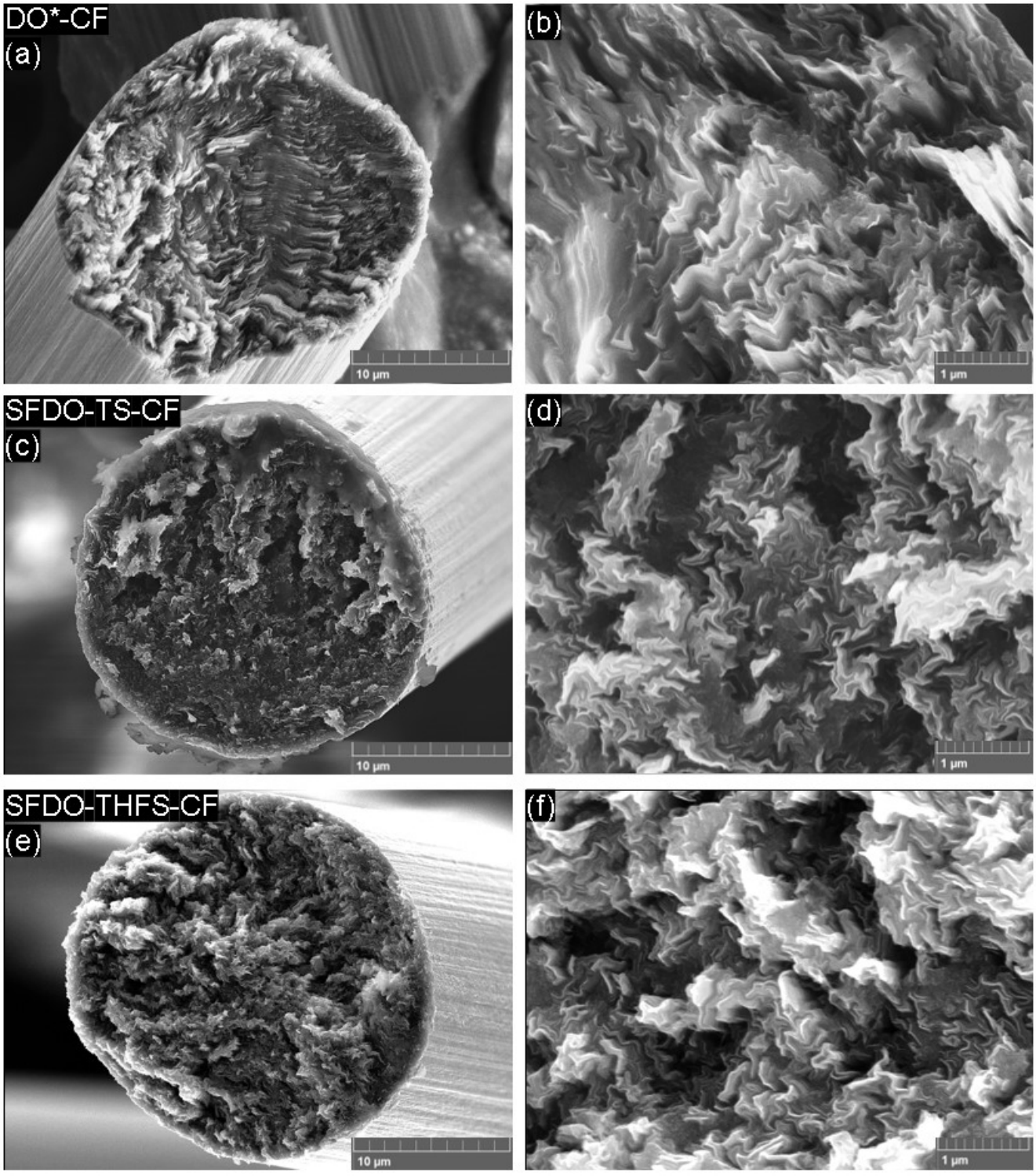

Figure 6. SEM images of cross-sections of DO*-CF (a,b), SFDO-TS-CF (c,d), and SFDO-THFS-CF (e,f).

The SFDO-derived graphitized fibers were tensile tested and the compliance corrected results were compared to those derived from DO* (Table 5). Carbon fiber originating from SFDO-TS and SFDO-THFS both showed a tensile modulus greater than 400 GPa, as well as higher strain to failure compared to DO*-CF. No significant difference in tensile properties was observed between SFDO-TS-CF and SFDO-THFS-CF. As expected, DO*-CF showed a tensile modulus of approximately 800 GPa, which is similar to previously reported tensile properties for DO-derived carbon fiber. [17, 19] The moduli results are consistent with the qualitative observations by SEM that SFDO-TS-CF and SFDO-THFS-CF appear to have smaller graphitic crystalline domains compared to DO*-CF (Figure 6).

Table 5. Compliance corrected tensile properties of mesophase pitch-derived carbon fiber.

	Diameter (μm)	Tensile modulus (GPa)	Break stress (MPa)	Break strain (%)
DO*-CF (n=56)	22.7 ± 2.2	795 ± 127	960 ± 460	0.12 ± 0.05
SFDO-TS-CF (n=78)	19.0 ± 2.5	479 ± 107	897 ± 363	0.19 ± 0.07
SFDO-THFS-CF (n=75)	23.2 ± 2.7	475 ± 94	943 ± 390	0.20 ± 0.07

Table 6. Crystallite dimensions of mesophase pitch-derived carbon fiber.

	d_{002} (Å)	L_c (Å)	N*
DO*-CF	3.389	286 ± 2	85
SFDO-TS-CF	3.398	187 ± 2	55
SFDO-THFS-CF	3.396	215 ± 2	63

*N is the average number of graphene sheets in the graphite crystallite, where $N=(L_c/d_{002})+1$.

Additionally, the d-spacing and crystallite size were obtained by XRD analysis to quantitatively explain the observed difference in tensile properties (Table 6). This data indeed suggests that DO*-CF had the largest graphitic crystallites in the c direction (L_c), corresponding to higher tensile modulus. The d_{002} spacing was also smallest for DO*-CF, which is consistent with it being the most graphitic. Conversely, the smaller crystallite sizes and larger d_{002} spacing observed in SFDO-TS-CF and SFDO-THFS-CF correspond to lower tensile modulus and higher break strain. Ultimately, the coal extract-derived carbon fiber may offer an advantageous combination of high modulus without being overly brittle. Furthermore, utilizing a coal extract

precursor can remarkably improve the overall yield of carbon fiber by approximately 70% relative to DO alone.

4. Conclusion

This work describes, for the first time, a process for utilizing raw coal for the production of high modulus carbon fiber. A coal extract precursor to mesophase pitch was obtained from direct coal liquefaction of Springfield coal in decant oil under mild conditions without high pressure, added catalyst, or H_2 gas. The coal extract showed higher asphaltene and preasphaltene content, alongside increased heteroatom content and a heavier and wider molecular weight range, compared to DO processed alone. Removal of insoluble residue was achieved via solvent dilution and filtration of the coal extract. THF was found to be the preferred dilution solvent due to its ability to effectively solubilize the coal-derived preasphaltenes.

The coal extracts were effectively converted to mesophase pitch in a one-pot thermal treatment approach without the need for an isotropic pitch intermediate. Furthermore, the coal extracts displayed notably higher thermal treatment yields relative to processed decant oil. These findings showcase that utilizing coal extracts from mild DCL is an attractive way to increase mesophase pitch yield while retaining properties amenable to melt spinning. Remarkably, coal utilization was shown to increase overall yield to mesophase pitch by nearly twofold and overall yield to carbon fiber by approximately 70% relative to processed decant oil alone. The coal-extract derived mesophase pitches were successfully melt-spun and thermally converted to graphitic carbon fiber with high modulus (> 400 GPa).

CRediT authorship contribution statement

Christina Thompson: Investigation, Data curation, Formal analysis, Visualization, Conceptualization, Writing - Original draft. **George Frank:** Investigation, Data curation, Formal analysis, Writing - Reviewing and editing. **Vivian Edwards:** Investigation, Data curation, Conceptualization, Writing - Reviewing and editing. **Michela Martinelli:** Investigation, Data curation, Conceptualization, Writing - Reviewing and editing. **Asmund Vego:** Investigation, Data curation, Conceptualization. **Frederic Vautard:** Resources, Investigation, Writing- Reviewing and editing. **Ercan Cakmak:** Resources, Investigation, Formal analysis. **John Craddock:** Project administration, Conceptualization, Writing- reviewing and editing. **Mark Meier:** Supervision,

Writing- reviewing and editing. **Rodney Andrews:** Funding acquisition, Supervision, Conceptualization. **Matthew Weisenberger:** Funding acquisition, Supervision, Conceptualization, Writing – review and editing.

Declaration of competing interests

Matthew Weisenberger, John Craddock, Christina Thompson, Asmund Vego, Vivian Edwards, Michela Martinelli, and Rodney Andrews have patent pending to University of Kentucky Research Foundation.

Acknowledgements

The authors thank Dr. David Eaton and Justin Lacy for assistance with mesophase production, as well as Kirk Norasak for carbon fiber thermal processing. This work was supported by the United States Department of Energy (FWP-FEAA155) Oak Ridge National Laboratory subcontract (40001811920), and by the University of Kentucky Center for Applied Energy Research.

References

(1) Newcomb, B. A. Processing, structure, and properties of carbon fibers. *Composites Part A: Applied Science and Manufacturing* **2016**, *91*, 262-282. DOI: 10.1016/j.compositesa.2016.10.018.
(2) Chand, S. Review Carbon fibers for composites. *Journal of Materials Science* **2000**, *35* (6), 1303-1313. DOI: 10.1023/A:1004780301489.
(3) Frank, E.; Steudle, L. M.; Ingildeev, D.; Spörl, J. M.; Buchmeiser, M. R. Carbon Fibers: Precursor Systems, Processing, Structure, and Properties. *Angewandte Chemie International Edition* **2014**, *53* (21), 5262-5298. DOI: 10.1002/anie.201306129.
(4) Das, S.; Warren, J.; West, D.; Schexnayder, S. M. *Global Carbon Fiber Composites Supply Chain Competitiveness Analysis*; Office of Scientific and Technical Information (OSTI), 2016. DOI: 10.2172/1260138.
(5) Arai, Y. *Structure and properties of pitch-based carbon fibers*; Nippon Steel Technical Report, 1993; pp 65-70.
(6) Mochida, I.; Shimizu, K.; Korai, Y.; Sakai, Y.; Fujiyama, S. Direct Preparation of Mesophase Pitch from Naphthalene by the Aid of HF/BF3. *Chemistry Letters* **1989**, *18* (11), 1893-1896. DOI: 10.1246/cl.1989.1893.
(7) Shimanoe, H.; Mashio, T.; Nakabayashi, K.; Inoue, T.; Hamaguchi, M.; Miyawaki, J.; Mochida, I.; Yoon, S.-H. Manufacturing spinnable mesophase pitch using direct coal extracted fraction and its derived mesophase pitch based carbon fiber. *Carbon* **2020**, *158*, 922-929. DOI: 10.1016/j.carbon.2019.11.082.
(8) Das, S.; Nagapurkar, P. *Sustainable Coal Tar Pitch Carbon Fiber Manufacturing*; United States, 2021. DOI: 10.2172/1784125.

(9) United States Department of Energy; National Energy Technology Laboratory. Carbon Ore Processing Program Project Portfolio, 2022.
(10) Mochida, I.; Okuma, O.; Yoon, S.-H. Chemicals from Direct Coal Liquefaction. *Chemical Reviews* **2014**, *114* (3), 1637-1672. DOI: 10.1021/cr4002885.
(11) Dadyburjor, D.; Biedler, P. R.; Chen, C.; Clendenin, L. M.; Katakdaunde, M.; Kennel, E. B.; King, N. D.; Magean, L.; Stansberry, P. G.; Stiller, A. H.; Zondlo, J. W. *PRODUCTION OF CARBON PRODUCTS USING A COAL EXTRACTION PROCESS*; United States, 2004. DOI: 10.2172/887333.
(12) Orchin, M.; Storch, H. H. Solvation and Hydrogenation of Coal. *Industrial & Engineering Chemistry* **1948**, *40* (8), 1385-1389. DOI: 10.1021/ie50464a010.
(13) Cakmak, E.; Hower, J. C.; Mathews, J. P.; Weisenberger, M. C.; Kaplan, R.; Lacy, J.; Zhang, Y.; Lara-Curzio, E. Microstructural diversity and digestion yields of select bituminous and subbituminous coals as raw material candidates for carbon fiber precursor production. *Fuel* **2023**, *348*, 128545. DOI: 10.1016/j.fuel.2023.128545.
(14) Kuznetsov, P. N.; Kamenskiy, E. S.; Kuznetsova, L. I. Solvolysis of Bituminous Coal in Coal- and Petroleum-Derived Commercial Solvents. *ACS Omega* **2020**, *5* (24), 14384-14393. DOI: 10.1021/acsomega.0c00915.
(15) Andrews, R. J.; Rantell, T.; Jacques, D.; Hower, J. C.; Steven Gardner, J.; Amick, M. Mild coal extraction for the production of anode coke from Blue Gem coal. *Fuel* **2010**, *89* (9), 2640-2647. DOI: 10.1016/j.fuel.2010.04.027.
(16) Oster, B.; Strege, J.; Kurz, M.; Snyder, A.; Jensen, M. *Subtask 3.3 - Feasibility of Direct Coal Liquefaction in the Modern Economic Climate*; United States, 2009. DOI: 10.2172/1001343.
(17) Wang, M.; Yang, B.; Yu, T.; Yu, X.; Rizwan, M.; Yuan, X.; Nie, X.; Zhou, X. Research progress in the preparation of mesophase pitch from fluid catalytic cracking slurry. *RSC Advances* **2023**, *13* (27), 18676-18689. DOI: 10.1039/D3RA01726E.
(18) Park, Y. D.; Korai, Y.; Mochida, I. Preparation of anisotropic mesophase pitch by carbonization under vacuum. *Journal of Materials Science* **1986**, *21* (2), 424-428. DOI: 10.1007/BF01145504.
(19) Guo, J.; Li, X.; Xu, H.; Zhu, H.; Li, B.; Westwood, A. Molecular Structure Control in Mesophase Pitch via Co-Carbonization of Coal Tar Pitch and Petroleum Pitch for Production of Carbon Fibers with Both High Mechanical Properties and Thermal Conductivity. *Energy & Fuels* **2020**, *34* (5), 6474-6482. DOI: 10.1021/acs.energyfuels.0c00196.
(20) Lou, B.; Liu, D.; Qiu, Y.; Fu, Y.; Guo, S.; Yu, R.; Gong, X.; Zhang, Z.; He, X. Modified effect on properties of mesophase pitch prepared from various two-stage thermotreatments of FCC decant oil. *Fuel* **2021**, *284*, 119034. DOI: 10.1016/j.fuel.2020.119034.
(21) Yan, T. Y.; Espenscheid, W. F. Liquefaction of coal in a petroleum fraction under mild conditions. *Fuel Processing Technology* **1983**, *7* (2), 121-133. DOI: 10.1016/0378-3820(83)90031-0.
(22) Martinelli, M.; Thompson, C. M.; Crowe, C. D.; Edwards, V. A.; Vego, A.; Craddock, J. D.; Meier, M. S.; Andrews, R.; Weisenberger, M. C. Elucidating the pathway of coal extract conversion to mesophase pitch via characterization of its feedstocks and isotropic intermediates. *Unpublished results submitted for publication* **2024**.
(23) Craddock, J. D.; Frank, G.; Martinelli, M.; Lacy, J.; Edwards, V.; Vego, A.; Thompson, C.; Andrews, R.; Weisenberger, M. C. Isotropic pitch-derived carbon fiber from waste coal. *Carbon* **2024**, *216*, 118590. DOI: 10.1016/j.carbon.2023.118590.

(24) Machnikowski, J.; Kaczmarska, H.; Leszczyńska, A.; Rutkowski, P.; Díez, M. A.; Álvarez, R.; García, R. Hydrogen-transfer ability of extrographic fractions of coal-tar pitch. *Fuel Processing Technology* **2001**, *69* (2), 107-126. DOI: 10.1016/S0378-3820(00)00139-9.
(25) Machnikowski, J.; Kaczmarska, H.; Gerus-Piasecka, I.; Díez, M. A.; Alvarez, R.; García, R. Structural modification of coal-tar pitch fractions during mild oxidation−relevance to carbonization behavior. *Carbon* **2002**, *40* (11), 1937-1947. DOI: 10.1016/S0008-6223(02)00029-5.
(26) Li, M.; Liu, D.; Lou, B.; Zhang, Y.; Yu, S.; Ding, J. Hydroalkylation modification of naphthene-based aromatic-rich fraction and its influences on mesophase development. *RSC Advances* **2018,** *8***,** 3750-3759. DOI: 10.1039/C7RA12619K.
(27) Morgan, T. J.; Alvarez-Rodriguez, P.; George, A.; Herod, A. A.; Kandiyoti, R. Characterization of Maya Crude Oil Maltenes and Asphaltenes in Terms of Structural Parameters Calculated from Nuclear Magnetic Resonance (NMR) Spectroscopy and Laser Desorption−Mass Spectroscopy (LD−MS). *Energy & Fuels* **2010**, *24* (7), 3977-3989. DOI: 10.1021/ef100320t.
(28) Zhang, C.; Lee, C. W.; Keogh, R. A.; Demirel, B.; Davis, B. H. Thermal and catalytic conversion of asphaltenes. *Fuel* **2001**, *80* (8), 1131-1146. DOI: 10.1016/S0016-2361(00)00178-2.
(29) Berkowitz, N.; Calderon, J.; Liron, A. Some observations respecting reaction paths in coal liquefaction: 1. Reactions of coal-tetralin slurries. *Fuel* **1988**, *67* (5), 626-631. DOI: 10.1016/0016-2361(88)90290-6.
(30) Mathews, J. P; Chaffee, A. L. The molecular representations of coal – A review. *Fuel* **2012**, *96*, 1–14. DOI: 10.1016/j.fuel.2011.11.025.
(31) Whitehurst, D. D.; Mitchell, T. O.; Farcasiu, M. The Composition of Coal. In *Coal Liquefaction: The Chemistry and Technology of Thermal Processes*; Academic Press, 1980; pp 6-27.
(32) Collins, C. J.; Raaen, V. F.; Benjamin, B. M.; Kabalka, G. W. Carbon-Carbon Cleavage During Asphaltene Formation. *Fuel* **1977**, *56*, 107. DOI: 10.1016/0016-2361(77)90051-5.
(33) Collins, C. J.; Benjamin, B. M.; Raaen, V. F.; Maupin, P. H.; and Roark, W. H. Isotopic Studies of Thermally Induced Reactions of Coal and Coal-Like Structures. In *Organic Chemistry of Coal,* ACS Symposium Series, Vol. 71; American Chemical Society, 1978; pp 165-170. DOI: 10.1021/bk-1978-0071.ch012.
(34) Wang, Z.; Zhao, Z.; Shui, H.; Ren, S.; Pan, C.; Lei, Z.; Kang, S.; Ge, Y.; Hu, J. Structural Characterization and Aggregation of the Subfractions of Preasphaltene from Direct Coal Liquefaction. *Energy & Fuels* **2014**, *28* (12), 7359-7367. DOI: 10.1021/ef501661f.
(35) Herod, A. A.; Zhuo, Y.; Kandiyoti, R. Size-exclusion chromatography of large molecules from coal liquids, petroleum residues, soots, biomass tars and humic substances. *Journal of Biochemical and Biophysical Methods* **2003**, *56* (1), 335-361. DOI: 10.1016/S0165-022X(03)00070-8.
(36) Karaca, F.; Islas, C. A.; Millan, M.; Behrouzi, M.; Morgan, T. J.; Herod, A. A.; Kandiyoti, R. The Calibration of Size Exclusion Chromatography Columns: Molecular Mass Distributions of Heavy Hydrocarbon Liquids. *Energy & Fuels* **2004**, *18* (3), 778-788. DOI: 10.1021/ef030178h.
(37) Wang, Z.; Li, L.; Shui, H.; Wang, Z.; Cui, X.; Ren, S.; Lei, Z.; Kang, S. Study on the aggregation of coal liquefied preasphaltene in organic solvents by UV–vis and fluorescence spectrophotometry. *Fuel* **2011**, *90* (1), 305-311. DOI: 10.1016/j.fuel.2010.08.009.

(38) Wang, Z.-C.; Ge, Y.; Shui, H.-F.; Ren, S.-B.; Pan, C.-X.; Kang, S.-G.; Lei, Z.-P.; Zhao, Z.-J.; Hu, J.-C. Molecular structure and size of asphaltene and preasphaltene from direct coal liquefaction. *Fuel Processing Technology* **2015**, *137*, 305-311. DOI: 10.1016/j.fuproc.2015.03.015.
(39) Kaminski, T. J.; Fogler, H. S.; Wolf, N.; Wattana, P.; Mairal, A. Classification of Asphaltenes via Fractionation and the Effect of Heteroatom Content on Dissolution Kinetics. *Energy & Fuels* **2000**, *14* (1), 25-30. DOI: 10.1021/ef990111n.
(40) Nalwaya, V.; Tantayakom, V.; Piumsomboon, P.; Fogler, S. Studies on Asphaltenes through Analysis of Polar Fractions. *Industrial & Engineering Chemistry Research* **1999**, *38* (3), 964-972. DOI: 10.1021/ie9804428.
(41) Taylor, G. H.; Pennock, G. M.; Gerald, J. D. F.; Brunckhorst, L. F. Influence of QI on mesophase structure. *Carbon* **1993**, *31* (2), 341-354. DOI: 10.1016/0008-6223(93)90039-D.
(42) Marsh, H.; Latham, C. S. The Chemistry of Mesophase Formation. In *Petroleum-Derived Carbons*, ACS Symposium Series, Vol. 303; American Chemical Society, 1986; pp 1-28.
(43) Mora, E.; Santamaría, R.; Blanco, C.; Granda, M.; Menéndez, R. Mesophase development in petroleum and coal-tar pitches and their blends. *Journal of Analytical and Applied Pyrolysis* **2003**, *68-69*, 409-424. DOI: 10.1016/S0165-2370(03)00034-2.
(44) Mochida, I.; Inoue, S.-I.; Maeda, K.; Takeshita, K. Carbonization of aromatic hydrocarbons—VI: Carbonization of heterocyclic compounds catalyzed by aluminum chloride. *Carbon* **1977**, *15* (1), 9-16. DOI: 10.1016/0008-6223(77)90068-9.
(45) Li, M.; Liu, D.; Men, Z.; Lou, B.; Yu, S.; Ding, J.; Cui, W. Effects of different extracted components from petroleum pitch on mesophase development. *Fuel* **2018**, *222*, 617-626. DOI: 10.1016/j.fuel.2018.03.011.
(46) Yang, J.; Wang, Z.; Liu, Z.; Zhang, Y. Novel Use of Residue from Direct Coal Liquefaction Process. *Energy & Fuels* **2009**, *23* (10), 4717-4722. DOI: 10.1021/ef9000083.
(47) Barraza, J.; Muñoz, N.; Barona, L. Asphaltenes and preasphaltenes from coal liquid extracts: feedstocks to obtain carbon mesophase. *Revista Facultad de Ingeniería Universidad de Antioquia* **2014**, *70*, 99-107. DOI: 10.17533/udea.redin.16169.
(48) Zhang, D.; Mu, C.; He, Y.; Lai, W.; Liu, H.; Liu, Q.; Yao, J.; Zhang, X.; Wang, X.; Xue, Z.; Nie, Y.; Song, K. Preparation and characterization of high performance coal tar pitch-based carbon fiber. *Fullerenes, nanotubes, and carbon nanostructures* **2024**, *32* (2), 128–140. DOI: 10.1080/1536383X.2023.2264417.
(49) Ramjee, S.; Rand, B.; Focke, W. W. Low shear rheological behaviour of two-phase mesophase pitch. *Carbon* **2015**, *82*, 368–380. DOI: 10.1016/j.carbon.2014.10.082.
(50) Honda H, Kimura H, Sanada Y, Sugawara S, Furuta T. Optical mesophase texture and X-ray diffraction pattern of the early-stage carbonization of pitches. *Carbon* **1970**, *8* (2), 181–189. DOI: 10.1016/0008-6223(70)90112-0.
(51) Kim, C. J.; Ryu, S. K.; Rhee, B. S. Properties of coal tar pitch-based mesophase separated by high-temperature centrifugation. *Carbon* **1993**, *31*, 833-838. DOI: 10.1016/0008-6223(93)90023-4.
(52) Liang, Z.; Lu, Y; Sun, Z.; Han, L. Polymerization kinetics and control of the components of a mesophase pitch. *New Carbon Materials* **2020**, *35* (5), 591-598. DOI: 10.1016/S1872-5805(20)60512-1.
(53) Li, M.; Liu, D.; Lv, R.; Ye, J.; Du, H. Preparation of the Mesophase Pitch by Hydrocracking Tail Oil from a Naphthenic Vacuum Residue. *Energy Fuels* **2015**, *29* (7), 4193–4200. DOI: 10.1021/acs.energyfuels.5b00537.

(54) Zha, Q.; Shi, J.; Ji, Y.; Liu, L.; Qian, S. The effect of composition and process variables on the spinnability of mesophase pitch. *Carbon* **1992**, *30* (5), 739-745. DOI: 10.1016/0008-6223(92)90156-Q.
(55) Guo, J.; Li, Z.; Li, B.; Chen, P.; Zhu, H.; Zhang, C.; Sun, B.; Dong, Z.; Li, X. Hydrogenation of coal tar pitch for improved mesophase pitch molecular orientation and carbon fiber processing. *Journal of Analytical and Applied Pyrolysis* **2023**, *174*, 106146. DOI: 10.1016/j.jaap.2023.106146.
(56) Yuan, G.; Xue, Z.; Cui, Z.; Westwood, A.; Dong, Z.; Cong, Y.; Zhang, J.; Zhu, H.; Li, X. Constructing the Bridge from Isotropic to Anisotropic Pitches for Preparing Pitch-Based Carbon Fibers with Tunable Structures and Properties. *ACS Omega* **2020**, *5* (34), 21948-21960. DOI: 10.1021/acsomega.0c03226.
(57) Chen, S.-L.; Ma, Z.-C.; Fan, C.-L.; Liang, Y.-L.; Ye, C. Study on spinning stability and microstructure of mesophase pitch. *Materials Express* **2020**, *10* (10), 1711-1717. DOI: 10.1166/mex.2020.1802.
(58) Weinberg, V. A.; Yen, T. F. Mesophase formation in coal liquid solvent fractions. *Carbon* **1983**, *21* (1), 39-45. DOI: 10.1016/0008-6223(83)90154-9.
(59) Świetlik, U.; Jasieńko, S.; Wolski, A. Carbonization and graphitization processes of pitch from coal liquid and its fractions. *Carbon* **1993**, *31* (3), 461-466. DOI: 10.1016/0008-6223(93)90134-V.
(60) Machnikowski, J. Kinetics and mechanism of carbonization of qi-free products from gas-coking coal hydrogenation-II. Carbonization of solvent fractions separated from coal hydrogenation pitches. *Carbon* **1993**, *31* (2), 373-381. DOI: 10.1016/0008-6223(93)90042-9.
(61) Young, L.-J. S.; Hara, T.; Li, N. C. Hydrogen bonding of the acid and base fractions separated from SRC II middle distillates. *Fuel* **1984**, *63* (6), 816-819. DOI: 10.1016/0016-2361(84)90073-5.
(62) Bockrath, B. C.; LaCount, R. B.; Noceti, R. P. Coal-derived asphaltenes: effect of phenol content and molecular weight on viscosity of solutions. *Fuel* **1980**, *59* (9), 621-626. DOI: 10.1016/0016-2361(80)90123-4.
(63) Marsh, H.; Mochida, I.; Macefield, I.; Scott, E. Carbonization and liquid-crystal (mesophase) development. 16. Carbonizations of soluble and insoluble fractions of coal-extract solution. *Fuel* **1980**, *59* (7), 514-516. DOI: 10.1016/0016-2361(80)90180-5.
(64) Marsh, H., Smith, J. The Formation and Properties of Anisotropic Cokes from Coals and Coal Derivatives Studied by Optical and Scanning Electron Microscopy. In *Analytical Methods for Coal and Coal Products*, Karr Jr., C. Ed.; Vol. II; Academic Press, 1978; pp 371-414.
(65) Jin, Z.; Zuo, X.; Long, X.; Cui, Z.; Yuan, G.; Dong, Z.; Zhang, J.; Cong, Y.; Li, X. Accelerating the oxidative stabilization of pitch fibers and improving the physical performance of carbon fibers by modifying naphthalene-based mesophase pitch with C9 resin. *Journal of Analytical and Applied Pyrolysis* **2021**, *154*, 105009. DOI: 10.1016/j.jaap.2020.105009.
(66) Yuan, G.; Li, B.; Li, X.; Dong, Z.; Hu, W.; Westwood, A.; Cong, Y.; Zhang, J. Effect of Liquid Crystalline Texture of Mesophase Pitches on the Structure and Property of Large-Diameter Carbon Fibers. *ACS Omega* **2019**, *4* (1), 1095-1102. DOI: 10.1021/acsomega.8b03189.